Seasonal variation and chemical characterization of PM$_{2.5}$ in northwestern Philippines

Gerry Bagtasa[1], Mylene G. Cayetano[1], and Chung-Shin Yuan[2]

[1]Institute of Environmental Science & Meteorology, University of the Philippines, Diliman, Quezon City, Philippines
[2]Institute of Environmental Engineering, National Sun-Yat Sen University, Kaoshiung, Taiwan ROC

Correspondence to: Gerry Bagtasa (gbagtasa@iesm.upd.edu.ph)

Abstract. The seasonal and chemical characteristics of fine particulate matter (PM$_{2.5}$) were investigated in Burgos, Ilocos Norte, located at the northwestern edge of the Philippines. Each 24H-sample of fine aerosol was collected for four seasons. Fine particulate in the region shows strong seasonal variation in both concentration and composition. Highest mass concentration was seen during the boreal spring season with a mean mass concentration of 21.6 ± 6.6 $\mu g\,m^{-3}$, and lowest was in fall with a mean concentration of 8.4 ± 2.3 $\mu g\,m^{-3}$. Three-day wind back trajectory analysis of air mass reveals the influence of the North Western Pacific monsoon regimes on PM$_{2.5}$ concentration. During southwest monsoon, sea salt was the dominant component of fine aerosols carried by moist air from the South China Sea. During northeast monsoon, on the other hand, both wind and receptor model analysis showed that higher particulate concentration was due to the long range transport (LRT) of anthropogenic emissions from northern East Asia. Overall, sea salt and soil comprise 33% of total PM$_{2.5}$ concentration while local biomass burning makes up 33%. LRT of industrial emission, solid waste burning and secondary sulfate from East Asia have a mean contribution of 34% to the total fine particulate for the whole sampling period.

1 Introduction

Increasing industrial emission and open burning of biomass and solid waste have shifted much interest in the local, regional and global transport of aerosol in Asia (Akimoto, 2003; Smith et al., 2011; Wang et al., 2014; Huang et al., 2013; Field and Shen, 2008). Aerosols are known not only for their impacts on health (Pope et al., 2002; Lelieveld et al., 2015; Jerrett, 2015; Silva et al., 2013), but also on their effects on Earth's energy budget (Ramanathan et al., 2013; Hansen et al., 1997; Chung et al., 2010). Its influence on the climate remains as one of the main uncertainties in our understanding of the atmosphere (IPCC, 2013). Rapid industrialization and urban development in the recent decades in Asia, particularly in mainland China, have led to an increase in energy consumption and consequently pollutant emissions. High emissions from the Asian main continent that are transported to other East Asian countries can contribute to elevated concentrations of ambient fine particulate elsewhere (Oh et al., 2015; Gu et al., 2016; Lin et al., 2014; Zhu et al., 2017; Cayetano et al., 2011). Similarly, biomass burning from land clearing in countries such as Indonesia and Malaysia has also affected their neighboring countries with reduced visibility and poor air quality (Aouizerats et al., 2015; Forsyth , 2014). Such events can have significant social, political and economic impacts on the region.

Aside from pollutant emission, meteorology plays a significant role in transboundary pollution. Certain weather patterns create transport pathways for long range transport (LRT) of gases and aerosols in the atmosphere. Outflow patterns of dusts and air pollutants can be induced from frontal lifting ahead of a southwestward moving cold front (Liu et al., 2003), or from two sequential low pressure systems interacting with a tropical warm sector (Itahashi et al., 2010) in East Asia. Also, the "warm conveyor belt" mechanism causes the seasonal uplifting and eventual transport of aerosols from East Asia to the free troposphere towards the Northwest Pacific (NWP) (Eckhardt et al., 2004). In the Southeast Asian (SEA) region, biomass burning in the maritime continent peaks during the spring season and is modulated by multi-scale meteorological factors such as El Niňo Southern Oscillation (ENSO), Inter-Tropical Convergence Zone (ITCZ) position, Indian Ocean Dipole (IOD), Madden-Julian Oscillation (MJO), monsoon winds and Tropical Cyclones (TC) (Field and Shen, 2008; Reid et al., 2015), the effects of which cover large regions of SEA. In certain instances, even reaching southern China and Taiwan (Lin et al., 2007, 2013). The Philippines have also been identified as a source of biomass burning emissions ubiquitous in SEA. Gadde et al. (2009) estimated an annual open field burning of 10.15 Tg of rice straw from 2002-2006 in the Philippines. This has led to observed elevated levels of levoglucosan and organic carbon (OC) at several sampling sites in Hong Kong during the springtime of 2004 and summer of 2006 where air parcels originating from the Pacific passed through the northern island of the Philippines (Sang et al., 2011; Ho et al., 2014). The life cycle of aerosols and their impacts on the regional climate system is the subject of several field campaigns across the region (i.e. 7-Seas (7-South-East Asian Studies), CAMPEX (Clouds, Aerosol, and Monsoon Processes-Philippines Experiment), YMC (Year of the Maritime Continent), BASE-ASIA (Biomass-burning Aerosols in South-East Asia: Smoke Impact Assessment), Fire Locating and Monitoring of Burning Emissions (FLAMBE)).

The region's complex meteorology, warm ocean water, high sensitivity to climate change and abundant aerosol sources create a complex aerosol-cloud-climate interaction that is still not well understood (Yusuf and Francisco, 2009; Reid et al., 2013). To the west of the Philippines, Reid et al. (2015) observed that the large-scale aerosol environment in the South China Sea (SCS) is modulated by MJO and TC activity in the NWP basin. TCs induce significant convective activity throughout the SCS that can extend for thousands of kilometers. The associated rainfall were seen as an effective means in aerosol scavenging that leads to low aerosol concentration despite numerous sources of emission in the region. Alternatively, high aerosol concentrations were observed along western Philippines during drier periods. To the east of the Philippines lies the Pacific "warm pool", which is among the warmest ocean area in the world (Comiso et al., 2015). The warm pool is also the main source of regional troposphere-to-stratospheric transported air (Fueglistaler et al., 2004). A study by Rex et al. (2014) reported the existence of a pronounced minimum in columnar ozone, as well as tropospheric column of the radical OH in the warm pool region. This will have implications on the global climate system as climate change may lead to an even warmer warm pool (Comiso et al 2015), and at the same time likely modify the abundance of OH (Hossaini et al., 2012). These factors may contribute in prolonging the lifetime of biomass burning-induced pollutants that can increase stratospheric intrusion in the future. Moreover, monsoon wind flows that influence regional climate and weather patterns also modulate aerosol transport. Using a chemical transport model WRF-CHEM, Bagtasa (2011) found that the two main monsoon regimes, northeast and southwest monsoon, mostly isolate the Philippines from East Asian pollution. However, northwesterly winds that can transport pollutants from southern China can be induced by TCs during its passage to the north or northeast of the Philippines.

There is limited literature on LRT aerosol observation in the country. This is perhaps due to the geographic separation of the Philippine archipelago from the Asian continent. The lack of observations in the northern Philippine region between the East Asian subtropics and the maritime continent of SEA makes this location a blind-spot in our knowledge of the current state of atmospheric environment. Also, satellite-based observations are hindered by persistent cloud cover over the region.

5　　This study aims to characterize the chemical composition of PM$_{2.5}$ on the northwest region of the Philippines, identify source contributions using a receptor model and investigate existing transport pathways in the NWP region. This paper will be presented as follows: the next section will detail the characteristics of the sampling site, aerosol sampling methodology, wind back trajectory and receptor modelling. The third section will discuss the influence of the NWP/Asian monsoon on the seasonal variability of observed concentrations of fine aerosol mass and its components, as well as emission sources derived

10　from meteorological and chemical receptor modeling. Finally, the last section will summarize the results of this study.

2 Methodology

2.1 Sampling site

Burgos (18.5° N, 120.57° E), a small town in the province of Ilocos Norte, is located in northwestern Luzon, northern Philippines as shown in figure 1. A filter-based air sampler (BGI PQ200, USA) was placed approximately 12 m above ground level

15　atop a 3-story building. The site is a rural environment surrounded by vegetation where the SCS (locally known as the West Philippine Sea) is 500 m to the west and a range of hills approximately 700 m to the east. A nearby road 100 m to the east is present, but has low daily traffic volume.

Burgos is classified as a Type 1 climate under the modified Coronas climate type classification (Coronas, 1912) where the region experiences wet season from May to September and a distinct dry season from October to April. Sampling during

20　summer (August - September) of 2015 coincided with a monsoon break, thus all sampling days for all seasons in the present study were non-rainy days and no synoptic disturbances (i.e. TC) were present. The area is also characterized by high winds during the boreal winter and spring seasons that is mainly attributed to the cornering effect of the northeast monsoon winds to Luzon Island.

2.2 Sample collection

25　Daily PM$_{2.5}$ samples were collected in August to September 2015, November 2015, January to February 2016 and March 2016 to represent the boreal summer, fall, winter and spring, respectively. Two-week (14 days) sampling was conducted for each season except for the summer sampling period when the northern region of the Philippines suffered provincial-wide power failure due to the effects of Typhoon Goni (locally named "Ineng"). Only seven days of sampling was done for summer. Table 1 summarizes the sampling dates of this study. Samples were collected using a 47 mm quartz fiber filter at a flow rate of 16.7

30　Lmin^{-1} from 1000H Philippines Standard Time (PST; +8 UTC) to 1000H PST the following day.

2.3 Chemical analysis

Prior to sampling, the quartz fiber filters are pre-heated at $900°$ C for 1.5 hours to remove impurities. Each filter is then weighed before and after sampling using a microbalance (Satorius MC5). The filter is then cut into four identical parts: one for the analysis of carbonaceous components, other parts for water-soluble ionic species, for metallic elements and for the analysis
5 of anhydrosugar.

Carbonaceous contents of $PM_{2.5}$ were measured using an elemental analyzer (Carlo Erba, Model 1108). The quarter part filter was divided into two, one part was heated with hot nitrogen gas (340-345° C) for 30 minutes to remove the OC fraction while the other part was analyzed without heating. The filter was then fed to the elemental analyzer to determine the amount of elemental carbon (EC) and total carbon (TC), respectively. OC concentration was calculated by getting the difference of
10 TC and EC. Another filter quarter was placed in a 15 ml polyethylene (PE) bottle filled with distilled and deionized water and subjected to ultrasonic extraction for 60 min, maintained at room temperature. Ion chromatography (DIONEX DX-120) was utilized to analyze the major anions (F^-, Br^-, Cl^-, SO_4^{2-} and NO_3^-) and cations (NH_4^+, Ca^{2+}, Na^+, K^+ and Mg^{2+}).

The last part of the filter was digested with a 30 ml mixed acid solution (HNO_3:$HCLO_4$, 3:7) at 150-200° C. After which the solution was diluted with 25 ml distilled and deionized water and stored in a PE bottle. Metallic elements (Al, As, Ca,
15 Cd, Cr, Cu, Fe, K, Mg, Mn, Ni, Pb, Ti, V and Zn) were determined using an Inductively Coupled Plasma-Atomic Emission Spectrometer (ICP-AES, Perkin Elmer, Optima 2000DV).

2.4 Wind and receptor modeling

Analysis of wind back trajectories was done using the HYSPLIT model (Draxler and Hess, 1998). Meteorological conditions were driven by output from Weather Research and Forecast (WRF) model (Skamarock et al., 2008) run with 5-day spin up time
20 for each sampling period. WRF model with spectral nudging was used to downscale the National Centers for Environmental Prediction or NCEP FNL (final) global reanalysis (downloaded from http://rda.ucar.edu) from 1° X 1° horizontal spatial resolution to 15 km resolution in a two-way nested domain of 45-15 km grid resolution. Twice-daily 72H back trajectories were then plotted and grouped into five clusters representing the general area of wind sources.

Receptor models are used to quantify the levels of air pollution, disaggregated into sources using statistical analysis of
25 particulate matter concentrations and its chemical components. Positive Matrix Factorization (PMF) is a widely used receptor model by the US Environmental Protection Agency (US EPA). The US EPA PMF has been applied to identify and apportion the air pollution sources in an industrial district of the capital city of Metro Manila, Philippines, in which lead (Pb) was found to have significant contributions in both coarse ($PM_{2.5-10}$) and fine ($PM_{2.5}$) particulate matter fractions (Pabroa et al., 2011). PMF is utilized in the present study to identify possible emission sources of observed fine aerosols.

3 Results and Discussion

3.1 Monsoon winds

The Philippines is categorized as a tropical rainforest / monsoon climate in the Köppen-Geiger climate classification. Its seasons are mainly described as wet or dry. The seasonality used in the present study mainly refers to the prevailing winds of the NWP/Asian monsoon, rather than changes in local temperature and rainfall as used in other climate classification methods. Figure 2 a-d show the prevailing winds (arrow), total accumulated rainfall (shading) and twice-daily 72H wind back trajectory (red line) in the NWP region during each of the four sampling periods. Averaged wind vectors are from the 6-hourly NCEP FNL reanalysis data and accumulated rainfall is from the TRMM 3B42A version 7 rainfall data product. Back trajectories are derived from the HYSPLIT-WRF simulations.

In the months of June-July-August (hereafter written as JJA, same for other seasons) or the boreal summer season, southwest monsoon wind prevails over western Philippines as shown in fig. 2a. The southwest monsoon period usually starts in the latter part of May and ends in September (Moron et al., 2009). The monsoon wind brings in warm moist air from the SCS, making the western coasts of the Philippines wet this season (Flores and Balagot, 1969; Bagtasa, 2017). SON or fall season in fig. 2b is marked by the southeast propagation of the ITCZ which results in the shifting of monsoonal winds from southwest to easterlies in September. This is followed by a shift to a northeasterly direction by the end of October or November (Bagtasa, 2017). Figure 2c shows northeast winds prevail during DJF or boreal winter. This season is also characterized by rainfall along the eastern coastal regions of the Philippines (Akasaka et al., 2007). Lastly, in fig. 2d, MAM (spring) marks the transition between northeast and southwest monsoon regimes. In this period, most convection stays near and south of the equator (Chang et al., 2005) with prevailing northeast to easterly winds from the Pacific Ocean.

The sampling periods in the present study were able to capture the climatological characteristics of each of the monsoon regimes for different boreal seasons. It is noteworthy that the northeast to southwest monsoon transition normally starts in the middle of March, but a late winter monsoon surge coincided with the spring sampling period. This presented a 'dry' northeast monsoon that had an influence on the observed spring aerosol concentration. Moreover, the years 2015 to early 2016 were strong El Niňo years, however, its influence on the NWP monsoon system will not be further discussed.

3.2 Seasonal variation of PM$_{2.5}$

The 24H PM$_{2.5}$ mass concentration shown in fig. 3 has a strong seasonal variation. PM$_{2.5}$ mass concentration for summer, fall, winter and spring had an average value and standard deviation of $11.9 \pm 5.0\,\mu\mathrm{g\,m^{-3}}$, $8.4 \pm 2.3\,\mu\mathrm{g\,m^{-3}}$, $12.9 \pm 4.6\,\mu\mathrm{g\,m^{-3}}$ and $21.6 \pm 6.6\,\mu\mathrm{g\,m^{-3}}$, respectively. The results show comparable concentrations measured from Dongsha Island in northern SCS except for heavy aerosol events previously reported in that site (Atwood, 2013; Lin et al., 2013). However, we expect aerosol sources in northern SCS to differ from our observations based on the MODIS-derived aerosol optical thickness (AOT) analysis of Lin et al. (2007). Their analysis showed northern SCS to be significantly influenced by emissions from southern and eastern China, which is not the case for northern Philippines based on our wind backtrajectory simulations. Carbonaceous components EC and OC in fig. 4 generally followed the same seasonal variation of PM$_{2.5}$. Minimum concentration was observed in fall

(EC 0.40 ± 0.09; OC 0.63 ± 0.18) in $\mu g\,m^{-3}$ and maximum in spring (EC 1.03 ± 0.21; OC 1.76 ± 0.39) in $\mu g\,m^{-3}$. The annual EC and OC mean concentration and standard deviation is $0.67 \pm 0.30\,\mu g\,m^{-3}$ and $1.15 \pm 0.63\,\mu g\,m^{-3}$, respectively. Measured EC likely originated from diesel buses and trucks that pass by the adjacent road. Traffic volume does not vary much near the sampling site. Hence, the small standard deviation observed. Overall, total carbon contribution to $PM_{2.5}$ is $13.4\% \pm 3.5\%$.

5   The mass ratio of the carbonaceous components OC/EC had been previously shown to determine contribution from primary or secondary sources (Chow et al., 1996). EC and OC are good tracers for fossil fuel combustion and biomass burning, respectively. EC is only of primary origin while OC may be emitted directly or form by gas-to-particle conversion in the atmosphere (Jones and Harrison, 2005). Accordingly, OC/EC ratio is usually used in source apportionment studies of carbonaceous aerosols (Pio et al., 2011). Figure 5 shows the seasonal average OC/EC mass ratio is 1.42, 1.74, 1.71 and 1.79 for summer,

10   fall, winter and spring season, respectively. Mean OC/EC ratio for all seasons are below the value of 2 which indicates that fine particulates are dominated by primary aerosol EC (Chow et al., 1996). On the basis of individual days, however, a third of the winter and spring data had values of OC/EC greater than 2.

3.2.1   Southwest Monsoon (Summer)

Upwind regions during southwest monsoon are known large aerosols emitters, particularly from biomass burning. However,

15   there is low observed aerosol concentration in this season. This is likely due to active convection around the island nations across the SCS (i.e. Borneo, Indochina peninsula) during the sampling period. Most air parcels indicated by the wind back trajectories originated from the marine boundary layer near these island regions. These air parcels were then transported along the western coast of northern Luzon before reaching the sampling site. The western coast of Luzon is characterized by substantial precipitation during the southwest monsoon season as a result of moist air being orographically lifted by the

20   Cordillera mountain range in western Luzon (Cayanan et al., 2011). An average accumulated rainfall of $91.2\,mm$ was recorded along northwestern Luzon coast throughout the seven day summer sampling period. These factors would have resulted in the suppression of biomass burning in the SEA region and scavenging of particulates along the path of the transported air parcels. In addition, the WRF simulation used to drive the HYSPLIT model showed a strong diurnal cycle of land/sea breeze along the western Luzon coasts. Nighttime land breeze carries polluted air from central and southwestern Luzon northwestward to the

25   SCS through Lingayen Gulf. After which, daytime sea breeze pushes back these polluted air masses inland along the northwest Luzon region. A similar land-sea breeze influence on the back-and-forth spatial distribution of pollutants was observed by Tsai et al. (2008) along the coastal region of Southern Taiwan.

3.2.2   Southwest to Northeast Monsoon transition (Fall)

November (fall) sampling showed the lowest mass concentrations among all seasons. During the fall monsoonal transition

30   regime, easterlies bring in air masses from the northwest Pacific Ocean (shown in fig. 2b) where no known large emission sources are present. Contribution from the eastern region of northern Philippines appears to be minimal as the northwest and northeast Philippines are separated by the northern hills of the Cordillera mountain range. Also, northeast Philippines is mainly composed of agricultural land with only little to moderate urban activities.

3.2.3 Northeast Monsoon (Winter and Spring)

Highest mass concentration is seen during spring time, followed by the winter observation. Strong northeasterly wind affected both sampling periods. Wind back trajectories of both seasons in fig. 2c and 2d show air parcels come from northern East Asia. However, better outflow patterns of pollutants from northern Asia during springtime may have contributed to higher observed mass concentrations in March. In addition, heavier precipitation from the Meiyu/Baiu front located along the East Asian subtropics during winter, as seen in fig. 2c, likely reduced the transported aerosols by wet scavenging before reaching the Philippines.

3.2.4 Wind trajectory cluster analysis

Figure 6 shows all the wind back trajectories grouped into five clusters. 17% (pink) of all simulated wind back trajectories occurred during southwest monsoon shows air parcels originated from the SCS and moved along the western coast of northern Luzon. In fall, 27% (blue) and 14% (red) originated from the near and far east Pacific, respectively. Total of 41% of pristine air parcels originated from the Pacific waters. This period is when the lowest $PM_{2.5}$ mass concentration including most of its components was observed. During northeast monsoon, 30% comes from northern East Asia and another 13% from East China sea. All five back trajectory clusters were simulated from ground to ground transport. The chemical characteristics and possible aerosol sources will be discussed in the following sections.

3.3 Ionic and metallic components

Figure 7 shows the seasonal mean and standard deviation of $PM_{2.5}$ and some water soluble ionic components. It is apparent that NO_3^-, SO_4^{2-} and NH_4^+ shown in fig. 7b, 7c and 7d , respectively, also follow the seasonal variation of $PM_{2.5}$ mass concentration. Minimum concentration was observed in fall and maximum during spring sampling. These three components are associated with secondary inorganic aerosol and make up on average 69% ± 4% of the total water soluble ions. Among all ionic species, SO_4^{2-} has the highest contribution at 2.43 ± 0.37 $\mu g\,m^{-3}$, followed by NO_3^- at 0.98 ± 0.25 $\mu g\,m^{-3}$ and NH_4^+ at 0.71 ± 0.14 $\mu g\,m^{-3}$. Seasonality of Na^+ with mean concentration of 0.37 ± 0.06 $\mu g\,m^{-3}$ and Ca^{2+} (0.34 ± 0.06 $\mu g\,m^{-3}$) also shows the same seasonal variability. However, this seasonality is not apparent for the ions Cl^-, K^+ and Mg^{2+}.

In fig. 7f, chlorine (Cl^-) summer sampling shows highest concentration of 0.69 ± 0.17 $\mu g\,m^{-3}$ and the rest of the seasons with nearly constant concentration of 0.52 ± 0.09 $\mu g\,m^{-3}$ for fall, 0.57 ± 0.07 $\mu g\,m^{-3}$ for winter and 0.60 ± 0.12 $\mu g\,m^{-3}$ for spring. We attribute the high Cl^- content in summer to sea salt carried by the southwest monsoon wind. Potassium (K^+) has mean concentration of 0.23 ± 0.06 $\mu g\,m^{-3}$. K^+ is a relatively abundant element in crustal rocks (Mason, 1966) and is also used as a tracer for wood burning due to its significant amount in wood biomass (Miles et al., 1996). Compared with levoglucosan measurements shown in table 2, K^+ is highly correlated to levoglucosan with correlation coefficient $r = 0.99$ at 95% confidence interval ($p < 0.05$). This indicates that measured K^+ is mainly from open burning of biomass, which is more widespread during the dry season of winter and spring. Magnesium (Mg^{2+}) has maximum concentration in spring and lowest in winter. For summer and fall, Mg^{2+} is highly correlated with Ca^{2+} (summer $r = 0.94$; fall $r = 0.97$, both at $p < 0.05$),

on the other hand, no significant correlation were found in other seasons. This suggests that the source of Mg^{2+} is mostly from mineral dust (carbonate mineral) when highly correlated with Ca^{2+} (Li et al., 2007). The high concentration of Mg^{2+} in spring is therefore attributed to non-local sources. Source attribution for these ions is further discussed in the results of receptor modeling in the next section.

5   Figure 8 shows some metallic components of measured fine particulates. Metallic components Al and Fe in figs. 8a and 8d, respectively, are associated with crustal origins (Mason, 1966). Seasonal variations of heavy metals Cd, Cr, Ni and Pb are shown in fig. 8b, 8c, 8e and 8f, respectively. Heavy metal components of fine particulates pose a health risk (Monaci et al 2000). Particularly, Ni, Cd and Cr are identified as human carcinogens while Pb is toxic and exposure can lead to permanent adverse health effects in humans (WHO, 1994). Dispersion of metals embedded in particulates also determines the rate at which metals

10 deposit on Earth's surface (Allen et al. , 2001). All heavy metal components were evidently high in spring, followed by the winter sampling period. Ambient concentrations of anthropogenic components depend on distance from source location and transport process (Thomaidis et al., 2003). Since no large industries or power plants are present within 250 km of the sampling site, these toxic components likely originated from upwind regions during northeast monsoon. No significant correlations were found between these metallic components with ionic components associated with secondary inorganic aerosols. This

15 suggests that these heavy metal components come from several different sources. Table 2 is the summary of the seasonal mean mass concentration and their corresponding standard deviation of $PM_{2.5}$ and its components, including the anhydrosugar levoglucosan.

     Figure 9a shows the ratio of cation and anion close to unity for all seasons (Figure 9 is in units of equivalent concentrations). This indicates good charge balance of atmospheric aerosols and high data quality used in the current study. Figure 9b shows

20 the scatter plot of Cl^- versus Na^+. The ratio Cl^-/Na^+ shows highest value in summer with 1.19, 1.08 for fall, 0.99 for winter and 0.89 for spring. The ratio indicates that summer Cl^- is mainly from sea salt where mean Cl^-/Na^+ ratio of sea salt is equivalent to 1.17 (Chester et al., 1990). This result supports our initial hypothesis that the high summer Cl^- concentration mainly comes from sea salt. In addition, there may be Cl^- depletion in the rest of the seasons due to the following factors: 1) farther distance from upwind coast (Dasgupta et al., 2007), 2) high sulfate and nitrate concentration during northeast monsoon

25 may have reacted with Cl^- in sea salt forming gas phase HCl in the process (Virkkula et al., 2006), and 3) excess Na^+ may have come from resuspended soil due to stronger wind in non-summer seasons. This is further supported by the high correlation values found between Fe and Al in winter ($r = 0.71$ at $p < 0.05$) and spring ($r = 0.88$ at $p < 0.05$) measurements which suggests higher loading of uplifted dust blown by strong winds during those seasons.

     Also mentioned in the previous section, Mg^{2+} is highly correlated with Ca^{2+} for summer and fall. This indicates mineral

30 dust as main source of Mg^{2+} in these seasons. In terms of the ratio of Mg^{2+}/Na^+, among all seasons, winter shows closest to the mean sea salt ratio of 0.23 (Chester, 1990), indicating mostly non-sea salt source for Mg except winter. Furthermore, ratio of both Mg^{2+}/Ca^{2+} and Mg^{2+}/Na^+ tends to vary more and spread out during spring season sampling as seen in graphs of fig. 9c and 9d. For the components associated with secondary inorganic aerosols, fig. 9e shows the ratio of NH_4^+/SO_4^{2-} all below unity (bold dashed line). The ratio points to NH_4^+ not fully neutralizing SO_4^{2-} all throughout the sampling periods. This

is possibly due to nearby sources of sea salt sulfate (S.S. SO_4^{2-}) in the region. Similarly, the ratio $NH_4^+/[NO_3^- + SO_4^{2-}]$ is also found to be below unity for all seasons. This suggests the presence of $NH_4^+NO_3^-$ as well as other forms of NO_3^- in the region.

3.4 Source contribution

The US EPA PMF 5.0 was used to resolve the contribution of the identified factor sources to the $PM_{2.5}$ concentration on each sampling day. The US EPA 5.0 uses a weighted least squares model, weighted based on known uncertainty or error of the elements of the data matrix (Paatero, 1999). The goal is to obtain the minimum Q value after several iterations, keeping the residuals at the most reasonable levels and having a sensible and rational factor profile. Details of the US EPA 5.0 are described elsewhere (Paatero, 1999; Paatero et al., 2002). Here, all 49 sampling datasets were used to resolve the factor and contribution profiles of $PM_{2.5}$ in northwestern Philippines. An extra 10% modeling uncertainty was added to the data to obtain the optimum convergence of the Q value and acceptable scaled residuals in the runs.

Here, we obtained 6 source factors namely: 1) sea salt, 2) resuspended fine dust, 3) local solid waste burning, 4) LRT of industrial emissions, 5) LRT solid waste burning and 6) LRT secondary sulfate. Figure 10 shows the profiles of the factors (sources) identified. Figure 11 shows the daily contribution per season for each of the source profiles. Using the source contributions, we were able to resolve the seasonal concentration of the sources, consistent with the factor profiles and fingerprints. For instance, elevated levels of sea salt contributed mainly during the summer season ($5.7 \pm 1.5\ \mu g\,m^{-3}$), consistent with our chemical analysis. On the other hand, LRT industrial emissions are observed at elevated levels during spring ($4.0 \pm 3.8\ \mu g\,m^{-3}$) and winter seasons ($3.1 \pm 2.7\ \mu g\,m^{-3}$), consistent with the chemical and wind back trajectory analysis discussed above. Table 3 summarizes the seasonal and total contribution of source factors to fine particulate matter of the region. Overall, natural primary sources sea salt and resuspended fine dust constitutes 33% of atmospheric aerosols. Another 33% or one third is due to local solid waste burning. This includes open burning of biomass in the dry season for the purpose of land clearing ubiquitous in SEA. Lastly, 34% is due to LRT sources from industrial emission, solid waste burning and secondary sulfate.

3.5 Enrichment factor

Analysis of the enrichment factor (Taylor , 1964; Hernández-Mena et al., 2011; Rushdi et al., 2013; Lomboy et al., 2015) is done to further characterize the composition and associations of the chemical components of $PM_{2.5}$. The analysis employs relating the concentration of $PM_{2.5}$ components that are known to be anthropogenic to those that are found stable in the crust, or those that are naturally found in the local atmosphere (Ackermann , 1980).

The enrichment factors of the chemical markers of identified sources are tabulated in Table 4. Factors associated with solid waste burning are divided into local and LRT burning factors. Both have high associations with K^+, Zn and OC. The LRT solid waste burning factor exhibits strong association with NO_3^-, NH_4^+, Mg^{2+}, Ca^{2+}, K^+, Zn, OC and EC. The enrichment factors of OC, EC, Zn and NO_3^- with respect to K^+ for local burning decreased to 50% when compared to the LRT counterpart, indicating the decrease in ageing of the $PM_{2.5}$ components as particles are transported over a long distance. The two other LRT factors identified, secondary sulfate and industrial factor source, showed strong associations with the heavy metals Cr, Ni, Cu, Cd and Pb. These chemical markers are reported in petroleum, chemical and manufacturing industries (Park et al.,

2002) that are not locally present. The secondary sulfate source marked an enrichment factor for $(Ca^{2+}+Mg^{2+})/Na^+$ of 5.7, which is about the same value as the enrichment factor of a certified reference material of China loess soil (Nishikawa et al., 2000), while that of the industrial emission factor (1.6) corresponds to the enrichment factor of sea salt ageing on processed dust particles from a marine background site in Korea (Cayetano et al., 2011).

5   It is noteworthy that significant contribution from long distance sources are observed during the northeast monsoon seasons of winter and spring. Analysis of wind back trajectory, PMF model and chemical components all demonstrate the existence of transboundary aerosols by way of the northeast monsoon wind. Furthermore, relatively lower concentration of components linked to LRT found in winter is likely modulated by rainfall associated with the Meiyu/Baiu front (shown in fig. 2c). More (less) frontal rain in winter (spring) resulted in increased (decreased) aerosol scavenging, which affected the overall transport

10   flow of LRT fine aerosols. Figure 12 shows a high correlation ($r = 0.87$) between the observed and reconstructed PMF-modeled $PM_{2.5}$ mass concentration, providing high confidence on the PMF analysis.

4   Conclusions

This study has described the seasonal characteristics of fine particulates ($PM_{2.5}$) in Burgos, Ilocos Norte, located in the north-western edge of the Philippines. This region is located between the East Asian subtropics and the maritime continent of SEA.

15   Both regions are known emitters of large quantities of anthropogenic aerosols. Observed fine particulates are mainly modu-lated by the NWP monsoon winds. $PM_{2.5}$ shows strong seasonality where the lowest mean concentration is found during fall season when easterly winds prevail. High concentrations were found in winter and spring time during the northeast monsoon season. $PM_{2.5}$ mass concentration for summer, fall, winter and spring had an average value and standard deviation of $11.9 \pm 5.0\,\mu g\,m^{-3}$, $8.4 \pm 2.3\,\mu g\,m^{-3}$, $12.9 \pm 4.6\,\mu g\,m^{-3}$ and $21.6 \pm 6.6\,\mu g\,m^{-3}$, respectively.

20   Components of fine particulates also showed distinct seasonality. Carbonaceous aerosol components EC and OC have an annual mean value of $0.67 \pm 0.30\,\mu g\,m^{-3}$ and $1.15 \pm 0.63\,\mu g\,m^{-3}$, respectively, both lowest in fall and highest in spring. EC and OC collectively make up $13.4\% \pm 3.5\%$ of observed fine particulates. The ionic and metallic components of fine aerosols also varied by sampling period which generally followed the seasonal variation of $PM_{2.5}$, and make up $44.4\% \pm 10.1\%$ and $11.7\% \pm 3.8\%$ of $PM_{2.5}$ mass, respectively. Analysis of the chemical components reveals high sea salt content in summer when

25   southwest monsoon winds prevail, and high concentration of components associated with secondary inorganic aerosols (i.e. NO_3^-, SO_4^{2-} and NH_4^+) as well as anthropogenic pollutants (i.e. heavy/toxic metals) during northeast monsoon. HYSPLIT-WRF wind back trajectory results show air masses originating from East Asia move along the northeasterly wind in winter and spring seasons. Winter sampling showed comparatively lower concentrations of $PM_{2.5}$ than spring. We attribute this to the scavenging of transported aerosols by the Meiyu/Baiu front, which had higher precipitation during the winter sampling period.

30   Positive Matrix Factorization (PMF) of the US EPA was used to determine the source contributors of fine particulate in the region. The results of the PMF receptor model and wind analysis were consistent and complementary. Here, six source profiles were obtained using the receptor model, namely: 1) sea salt, 2) resuspended fine dust, 2) local solid waste burning, 4) LRT of industrial emissions, 5) LRT solid waste burning and 6) LRT secondary sulfate. Consistent with the chemical analysis, high

sea salt in summer contributes to almost half of aerosol content for that season. Resuspended fine dust is seen to increase in the spring and winter season when strong winds prevail over the sampling site. Open burning of biomass and solid waste is widespread in the dry seasons of winter and spring. This is seen in the seasonality of K^+ and the anhydrosugar levoglucosan, which were found to be highly correlated with one another. LRT of anthropogenic fine particulates were observed during winter and spring time when the northeast monsoon serves as transport pathway for East Asian aerosols to reach the northern part of the Philippines. The annual mean source contribution of transboundary industrial emission, secondary sulfate and solid waste burning was 14%, 9% and 11%, respectively. In total, LRT contributes to one third of aerosol content in the region.

To our knowledge, this is the first comprehensive analysis of aerosol characteristics in this region of the Philippines. Also, this is the first study to confirm long range transport of East Asian aerosols to the country. It would be interesting to see its implications on the region's radiative forcing, aerosol-cloud-climate interaction and stratospheric intrusion, if there are any. These are questions essential to a better understanding of the region's atmosphere.

References

Ackermann, F.: A procedure for correcting the grain size effect in heavy metal analyses of estuarine and coastal sediments. Environmental Technology, 1(11), pp.518-527, 1980.

Akasaka, I., Morishima, W., and Mikami, T.: Seasonal march and its spatial difference of rainfall in the Philippines. Int. J. Climatol., 27, 715–7252, doi:10.1002/joc.1428, 2007.

Akimoto, H.: Global Air Quality and Pollution, Science 302, 1716, doi:10.1126/science.1092666, 2003.

Allen, A.G., Nemitz, E., Shi, J.P., Harrison, R.M., and Greenwood, J.C.: Size distributions of trace metals in atmospheric aerosols in the United Kingdom, Atmospheric Environment 35 (27), 4581–4591, 2001.

Aouizerats, B., van der Werf, G. R., Balasubramanian, R., and Betha, R.: Importance of transboundary transport of biomass burning emissions to regional air quality in Southeast Asia during a high fire event, Atmos. Chem. Phys., 15, 363-373, doi:10.5194/acp-15-363-2015, 2015.

Atwood, S. A., Reid, J. S., Kreidenweis, S. M., Cliff, S. S., Zhao, Y., Lin, N.-H., Tsay, S.-C., Chu, Y.-C., Westphal, D. L.: Size resolved measurements of springtime aerosol particles over the northern South China Sea, In Atmospheric Environment, Vol. 78, pp. 134-143, ISSN 1352-2310, doi:10.1016/j.atmosenv.2012.11.024, 2013.

Bagtasa, G.: Effect of synoptic scale weather disturbance to Philippine transboundary ozone pollution using WRF-CHEM, Internation journal on Environmental Science and Development, Vol. 3 No. 5, 2011.

Bagtasa, G.: Contribution of Tropical Cyclones to Rainfall in the Philippines, J. Climate,30,3621-3633, doi:10.1175/JCLI-D-16-0150.1, 2017

Cayanan, E. O., Chen, T.-C., Argete, J. C., Yen, M.-C., and Nilo, P. D.: The effect of tropical cyclones on southwest monsoon rainfall in the Philippines, J. Meteor. Soc. Japan, 89A, 123–139, doi:10.2151/jmsj.2011-A08, 2011.

Cayetano, M. G., Kim, Y. J., Jung, J., Batmunkh, T., Lee, K.Y., Kim, S.Y., Kim, K.C., Kim, D.G., Lee, S.J., Kim, J.S., and Chang, L.S.: Observed Chemical Characteristics of long-range transported particles at a marine background site in Korea. Journal of Air and Waste Management Association , 61 (11), 1192-1203, 2011.

Cayetano, M.G., Hopke, P.K., Lee, K.H., Jung, J., Batmunkh, T., Lee, K., and Kim, Y.J.: Investigations of the particle compositions of transported and local emissions in Korea, Aerosol and Air Quality Research, 14, 793-805, 2014.

Chang, C.-P., Wang, Z., McBride, J., and Liu, C.-H.: Annual cycle of Southeast Asia maritime continent rainfall and the asymmetric monsoon transition, J. Climate, 18, 287–301, doi:10.1175/JCLI-3257.1, 2005.

Chester R., Nimmo, M., Murphy, K.J.T., and Nicholas, E.: Atmospheric trace metals transported to the Western Mediterranean: data from a station on Cap Ferrat, Water Pollution Reports, 20, J.-M. Martin and H. Barth, editors. Commission of the European Communities, 597-612, 1990.

Chow, J. C., Watson, J. G., Lu, Z., Lowenthal, D. H., Frazier, C. A., Solomon, P. A., and Thuillier, R. H.: Descriptive analysis of $PM_{2.5}$ and PM_{10} at regionally representative locations during SJVAQS/AUSPEX, Atmos. Environ., 30, 2079–2112, 1996.

Chung, C. E., Ramanathan, V., Carmichael, G., Kulkarni, S., Tang, Y., Adhikary, B., Leung, L. R., and Qian, Y.: Anthropogenic aerosol radiative forcing in Asia derived from regional models with atmospheric and aerosol data assimilation, Atmos. Chem. Phys., 10, 6007-6024, doi:10.5194/acp-10-6007-2010, 2010.

Comiso, J.C., Perez, G.P., and Stock, L.V.: Enhanced Pacific Ocean Sea Surface Temperature and Its Relation to Typhoon Haiyan, J. of Environmental Science and Management, Vol. 18 No. 1, 2015.

Coronas, J.: The extraordinary drought in the Philippines: October, 1911, to May, 1912, Weather Bureau, Department of the Interior, Government of the Philippine Islands, 1912.

Dasgupta, P.K., Campbell, S.W., Al-Horr, R.S., Rahmat Ullah, S.M., Li, J., Amalfitano, C., and Poor, N.D.:Conversion of sea salt aerosol to NaNO$_3$ and the production of HCl: Analysis of temporal behavior of aerosol chloride/nitrate and gaseous HCl/HNO$_3$ concentrations with AIM, Atmos Environ 41: 4242–4257, 2007.

Draxler, R.R. and Hess, G.D.: An Overview of the Hysplit4 Modeling System for Trajectories, Dispersion, and Deposition, Aust. Met. Mag., 47, 295-308, 1998.

Eckhardt, S., Stohl, A., Wernli, H., James, P., Forster, C.,and Spichtinger, N.: A 15-year climatology of warm conveyor belts, J. Climate, 17, 218–237, doi:10.1175/1520-0442(2004)017<0218:AYCOWC>2.0.CO;2, 2004.

Field, R.D. and Shen, S.S.P.: Predictability of carbon emissions from biomass burning in Indonesia, J. Geophys. Res., 113, p. G04024, 10.1029/2008JG000694, 2008.

Flores, J., V. and Balagot, V.: Climate of the Philippines. Climates of Northern and Eastern Asia, H. Arakawa, Ed., World Survey of Climatology, Vol. 8. Elsevier, 159–213, 1969.

Forsyth, T.: Public Concerns About Transboundary Haze: A Comparison Of Indonesia, Singapore, And Malaysia, Global Environmental Change 25, 76–86,2014.

Fueglistaler, S., Wernli, H., and Peter, T.: Tropical troposphere-to-stratosphere transport inferred from trajectory calculations, J. Geophys. Res., 109, D03108, doi:10.1029/2003JD004069, 2004.

Gadde, B., Bonnet, S., Menke, C., and Garivait, S.: Air pollutant emissions from rice straw open field burning in India, Thailand and the Philippines, Environ. Pollut., 157 (5), 1554-1558, 2009.

Gu, Y., and Yim, S.H.L.: The air quality and health impacts of domestic trans-boundary pollution in various regions of China. Environment International 97, 117-124, 2016.

Hansen, J., Sato, M., and Ruedy, R.: Radiative forcing and climate response, J. Geophys. Res., 102, 6831–6864, doi:10.1029/96JD03436, 1997.

Hernández-Mena, L., Murillo-Tovar, M., Ramírez-Muñíz, M., Colunga-Urbina, E., de la Garza-Rodríguez, I. and Saldarriaga-Noreña, H.: Enrichment factor and profiles of elemental composition of PM 2.5 in the city of Guadalajara, Mexico. Bulletin of environmental contamination and toxicology, 87(5), p.545, 2011.

Ho, K.F., Engling, G., Ho, S.S.H., Huang, R., Lai, S.C., Cao, J., and Lee, C.S.: Seasonal variations of anhydrosugars in PM 2.5 in the Pearl River Delta Region, China, Tellus. Series B, Chemical and physical meteorology, 2014, v. 66, p. 1-14, 2014.

Hossaini, R., Chipperfield, M. P., Dhomse, S., Ordóñez, C., Saiz-Lopez, A., Abraham, N. L., Archibald, A., Braesicke, P., Telford, P., Warwick, N., Yang, X., and Pyle, J.: Modelling future changes to the stratospheric source gas injection of biogenic bromocarbons, Geophys. Res. Lett., 39, L20813, doi:10.1029/2012GL053401, 2012.

Huang, K., Fu, J.S., Hsu, N.C., Gao, Y., Dong, X., Tsay, S.C., and Lam, Y.F.: Impact assessment of biomass burning on air quality in Southeast and East Asia during BASE-ASIA, Atmospheric Environment 78, 291-302, 2013.

IPCC: Intergovernmental Panel on Climate Change. Fifth Assessment Report. Cambridge University Press, Cambridge, United Kingdom and New York, NY, USA, 1535 pp, doi:10.1017/CBO9781107415324., 2013.

Itahashi, S., K. Yumimoto, I. Uno, K. Eguchi, T. Takemura, Y. Hara, A. Shimizu, N. Sugimoto, and Z. Liu: Structure of dust and air pollutant outflow over East Asia in the spring, Geophys. Res. Lett., 37, L20806, doi:10.1029/2010GL044776, 2010.

Jerrett, M.: Atmospheric science: The death toll from air-pollution sources, Nature 525, 330–331, doi:10.1038/525330a, 2015.

Jones, A.M. and Harrison, R.M.: Interpretation of particulate elemental and organic carbon concentrations at rural, urban and kerbside sites. Atmospheric Environment, 39(37), pp.7114-7126, 2005.

Lelieveld, J., Evans, J. S., Fnais, M., Giannadaki, D., and Pozzer, A.: The contribution of outdoor air pollution sources to premature mortality on a global scale, Nature 525, 367–371. doi:10.1038/nature15371, 2015.

Li, G., Chen, J., Chen, Y., Yang, J., Ji, J., and Liu, L.: Dolomite as a tracer for the source regions of Asian dust, J. Geophys. Res., 112, D17201, doi:10.1029/2007JD008676, 2007.

5 Lin, I.-I., Chen, J.-P., Wong, G.T.F., Huang, C.-W., Lien, C.-C.: Aerosol input to the South China Sea: Results from the MODerate Resolution Imaging Spectro-radiometer, the Quick Scatterometer, and the Measurements of Pollution in the Troposphere Sensor, In Deep Sea Research Part II: Topical Studies in Oceanography, Vol. 54, Issues 14–15, pp 1589-1601, ISSN 0967-0645, doi:10.1016/j.dsr2.2007.05.013, 2007.

Lin, N.-H., Si-Chee Tsay, S.-C., Maring, H. B., Yen, M.-C. Sheu, G.-R., Wang, S.-H., Chi, K.-H., Chuang, M.-T., Ou-Yang, C.-F., Fu, J. S.,
10 Reid, J. S., Lee, C.-T., Wang, L.-C., Wang, J.-L., Hsu, C. N., Sayer, A. M., Holben, B. N., Yu-Chi Chu, Y.-C., Nguyen, X. A., Sopajaree, K., Chen, S.-J., Cheng, M.-T., Tsuang, B. J., Tsai, C.-J., Peng, C.-M., Schnell, R. C., Conway, T., Chang, C.-T., Lin, K.-S., Tsai, Y. I., Lee, W.-J., Chang, S.-C., Liu, J.-J., Chiang, W.-L., Huang, S.-J., Lin, T.-H., and Liu, G. R.: An overview of regional experiments on biomass burning aerosols and related pollutants in Southeast Asia: From BASE-ASIA and the Dongsha Experiment to 7-SEAS, Atmos. Environ., 78, 1–19, doi:10.1016/j.atmosenv.2013.04.066, 2013.

15 Lin, J., Pan, D., Davis, S.J., Zhang, Q., He, K., Wang, C., Streets, D.G., Wuebbles, D.J., and Guan, D.: China's international trade and air pollution in the United States, PNAS vol. 111 no. 5. 1736–1741, doi: 10.1073/pnas.1312860111, 2014.

Liu, H., Jacob, D.J., Bey, I., Yantosca, R.M., Duncan, B.N., and Sachse, G.W.: Transport pathways for Asian pollution outflow over the Pacific: Interannual and seasonal variations, J. Geophys. Res., 108(D20), 8786, doi:10.1029/2002JD003102, 2003

Lomboy, M.F.T.C., Quirit, L.L., Molina, V.B., Dalmacion, G.V., Schwartz, J.D., Suh, H.H. and Baja, E.S.: Characterization of particulate
20 matter 2.5 in an urban tertiary care hospital in the Philippines. Building and Environment, 92, pp.432-439, 2015.

Mason, B., 1966: Principles of Geochemistry. Wiley, New York.

Miles, T. R., Miles, T.R., Baxter, L.L., Bryers, R.W., Jenkins, B.M., and Oden, L.L.: Boiler deposits from firing biomass fuels, Biomass and Bioenergy 10, 25-138, 1996.

Monaci, F., Moni, F., Lanciotti, E., Grechi, D., and Bargagli, R.: Biomonitoring of airborne metals in urban environments: new tracers of
25 vehicle emissions, in place of lead, Environ Pollut. 2000; 107: 321–327 pmid:15092978, 2000.

Moron, V., Lucero, A., Hilario, F., Lyon, B., Robertson, A., and DeWitt, D.: Spatio-temporal variability and predictability of summer monsoon onset over the Philippines, Climate Dyn., 33, doi:10.1007/s00382-008-0520-5, 2009.

Nishikawa, M., Hao, Q., and Morita, M.: Preparation and evaluation of certified reference materials for Asian mineral dust, Global Environ. Res., 4, 103 – 113, 2000.

30 Oh, H.R., Ho,C.H., Kim,J., Chen, D., Lee,S., Choi,Y.S., Chang, L.S., and Song, C.K.: Long-range transport of air pollutants originating in China: A possible major cause of multi-day high-PM10 episodes during cold season in Seoul, Korea, Atmospheric Environment. Volume 109, May 2015, Pages 23-30, 2015.

Paatero, P.: The multilinear engine - a table-driven, least squares program for solving multilinear problems, including the n-way parallel factor analysis model. Journal of Computational and Graphical Statistics , 8 (4), 854-888, 1999.

35 Paatero, P., Hopke, P., Song, H., and Ramadan, Z.: Understanding and controlling rotations in factor analytic models. Chemometrics and intelligent laboratory systems , 60 (1-2), 253-264, 2002.

Pabroa, P.C.B., Santos, F.L., Morco, R.P., Racho, J.M.D., Bautista, A.T., and Bucal, C.G.D.: Receptor modeling studies for the characterization of air particulate lead pollution sources in Valenzuela sampling site (Philippines), Atmospheric Pollution Research. Volume 2, Issue 2, April 2011, 213-218, 2011.

Park, H., Chah , E., Choi, H., Kim, H., and Yi, J. : Releases and transfers from petroleum and chemical manufacturing industries in Korea, Atmospheric Environment , 36 (31), 4851-4861, 2002.

Pio, C., Cerqueira, M., Harrison, R.M., Nunes, T., Mirante, F., Alves, C., Oliveira, C., de la Campa, A.S., Artíñano, B. and Matos, M.: OC/EC ratio observations in Europe: Re-thinking the approach for apportionment between primary and secondary organic carbon. Atmospheric Environment, 45(34), pp.6121-6132, 2011.

Pope, C. A., Burnett, R.T., and Thun, M.J.: Lung Cancer, Cardiopulmonary Mortality, and Long-term Exposure to Fine Particulate Air Pollution, Journal of American Medical Association , 287 (9), 1132-1141, 2002.

Ramanathan, V., Callis, L., Cess, R., Hansen, J., Isaksen, I., Kuhn, W., Lacis, A., Luther, F., Mahlman, J., and Reck, R.: Climate-chemical interactions and effects of changing atmospheric trace gases, Schlesinger, 1987.

Reid, J. S., Hyer, E. J., Johnson, R. S., Holben, B. N., Yokelson, R. J., Zhang, J., Campbell, J. R., Christopher, S. A., Di Girolamo, L., Giglio, L., Holz, R. E., Kearney, C., Miettinen, J., Reid, E. A., Turk, F. J., Wang, J., Xian, P., Zhao, G., Balasubramanian, R., Chew, B. N., Janjai, S., Lagrosas, N., Lestari, P., Lin, N. H., Mahmud, M., Nguyen, A. X., Norris, B., Oanh, N. T. K., Oo, M., Salinas, S. V., Welton, E. J., and Liew, S. C.: Observing and understanding the Southeast Asian aerosol system by remote sensing: An initial review and analysis for the Seven Southeast Asian Studies (7SEAS) program, Atmos. Res., 122, 403–468, doi:10.1016/j.atmosres.2012.06.005, 2013.

Reid, J. S., Lagrosas, N. D., Jonsson, H. H., Reid, E. A., Sessions, W. R., Simpas, J. B., Uy, S. N., Boyd, T. J., Atwood, S. A., Blake, D. R., Campbell, J. R., Cliff, S. S., Holben, B. N., Holz, R. E., Hyer, E. J., Lynch, P., Meinardi, S., Posselt, D. J., Richardson, K. A., Salinas, S. V., Smirnov, A., Wang, Q., Yu, L., and Zhang, J.: Observations of the temporal variability in aerosol properties and their relationships to meteorology in the summer monsoonal South China Sea/East Sea: the scale-dependent role of monsoonal flows, the Madden–Julian Oscillation, tropical cyclones, squall lines and cold pools, Atmos. Chem. Phys., 15, 1745–1768, doi:10.5194/acp-15-1745-2015, 2015.

Rex, M., Wohltmann, I., Ridder, T., Lehmann, R., Rosenlof, K., Wennberg, P., Weisenstein, D., Notholt, J., Krüger, K., Mohr, V., and Tegtmeier, S.: A tropical West Pacific OH minimum and implications for stratospheric composition, Atmos. Chem. Phys., 14, 4827-4841, doi:10.5194/acp-14-4827-2014, 2014.

Rushdi, A.I., Al-Mutlaq, K.F., Al-Otaibi, M., El-Mubarak, A.H. and Simoneit, B.R.: Air quality and elemental enrichment factors of aerosol particulate matter in Riyadh City, Saudi Arabia. Arabian Journal of Geosciences, 6(2), pp.585-599, 2013.

Sang, X., Chan, C.Y., Engling, G., Chan, L.Y., Wang, X.M., Zhang, Y.N., Shi, S., Zhang, Z.S., Zhang, T. and Hu, M.: Levoglucosan enhancement in ambient aerosol during springtime transport events of biomass burning smoke to Southeast China, Tellus B , 63 (B), 129-139, 2011.

Silva,R.A., West,J.J., Zhang, Y., Anenberg,S.C., Lamarque,J.F., Shindell,D.T., Collins, W.J., Dalsoren, S., Faluvegi,G. , Folberth, G., Horowitz, L.W., Nagashima, T., Naik,V. , Rumbold,S. , Skeie,R. , Sudo,K. , Takemura,T. , Bergmann,D. , Smith,P.C. , Cionni,I. , Doherty,R.M. , Eyring,V. , Josse,B. , MacKenzie,I.A. , Plummer,D. , Righi,M. , Stevenson,D.S. , Strode, S., Szopa, S., and Zeng, G.: Global premature mortality due to anthropogenic outdoor air pollution and the contribution of past climate change, Environ. Res. Lett. 8, doi:10.1088/1748-9326/8/3/034005, 2013.

Skamarock, W. C., Klemp, J.B., Dudhia. J., Gill, D.O., Barker, D., Wang, W., and Powers, J.G.: A description of the Advanced Research WRF version 3. NCAR Tech. Note NCAR/TN-475+STR, 2008.

Table 1. Sampling dates

Season	Sampling dates	Sampling days
Summer	Aug. 27 - Sept. 2, 2015	7
Fall	Nov. 5 - Nov. 18, 2015	14
Winter	Jan. 21 - Feb. 3, 2016	14
Spring	Mar. 17 - Mar. 30, 2016	14

Smith, S. J., J. van Aardenne, Z. Klimont, R. J. Andres, A. Volke, and S. Delgado Arias: Anthropogenic sulfur dioxide emissions: 1850–2005, Atmos. Chem. Phys., 11, 1101–1116, doi:10.5194/acp-11-1101-2011, 2011

Taylor, S.R.: Abundance of chemical elements in the continental crust: a new table. Geochimica et cosmochimica acta, 28(8), pp.1273-1285, 1964.

5   Thomaidis, N.S., Bakeas, E.B., and Siskos, P.A.: Characterization of lead, cadmium, arsenic and nickel particles in the Athens atmosphere, Greece, Chemosphere 52, 959-966, 2003.

Tsai, H.H., Ti, T.H., Yuan, C.S., Hung, C.H. and Lin, C.: Effects of sea-land breezes on the spatial and temporal distribution of gaseous air pollutants at the coastal region of southern Taiwan. J. Environ. Eng. Manag, 18, pp.387-396, 2008.

Virkkula, A., Saarikoski, S., Aurela, M., and Kulmala, M.: Chemical size distributions of boundary layer aerosol over the Atlantic Ocean and at an Antarctic site, J. Geophys. Res. Atmos., 111, D05306, 2006.

10   Wang, S. X., Zhao, B., Cai, S. Y., Klimont, Z., Nielsen, C. P., Morikawa, T., Woo, J. H., Kim, Y., Fu, X., Xu, J. Y., Hao, J. M., and He, K. B.: Emission trends and mitigation options for air pollutants in East Asia, Atmos. Chem. Phys., 14, 6571-6603, doi:10.5194/acp-14-6571-2014, 2014.

World Health Organization: International Agency for Research on Cancer. Monographs volumes 1–60, 1972–1994 and Supplement 7 1987, World Health Organization, Geneva, 1994.

15   Yusuf, A.A. and Francisco, H.: Climate Change Vulnerability Mapping for Southeast Asia, Economy and Environment Program for Southeast Asia, 2009

Zhu, J., Liao, H., Mao, Y., Yang, Y., and Jiang, H.: Interannual variation, decadal trend, and future change in ozone outflow from East Asia, Atmos. Chem. Phys., 17, 3729–3747, doi:10.5194/acp-17-3729-2017, 2017.
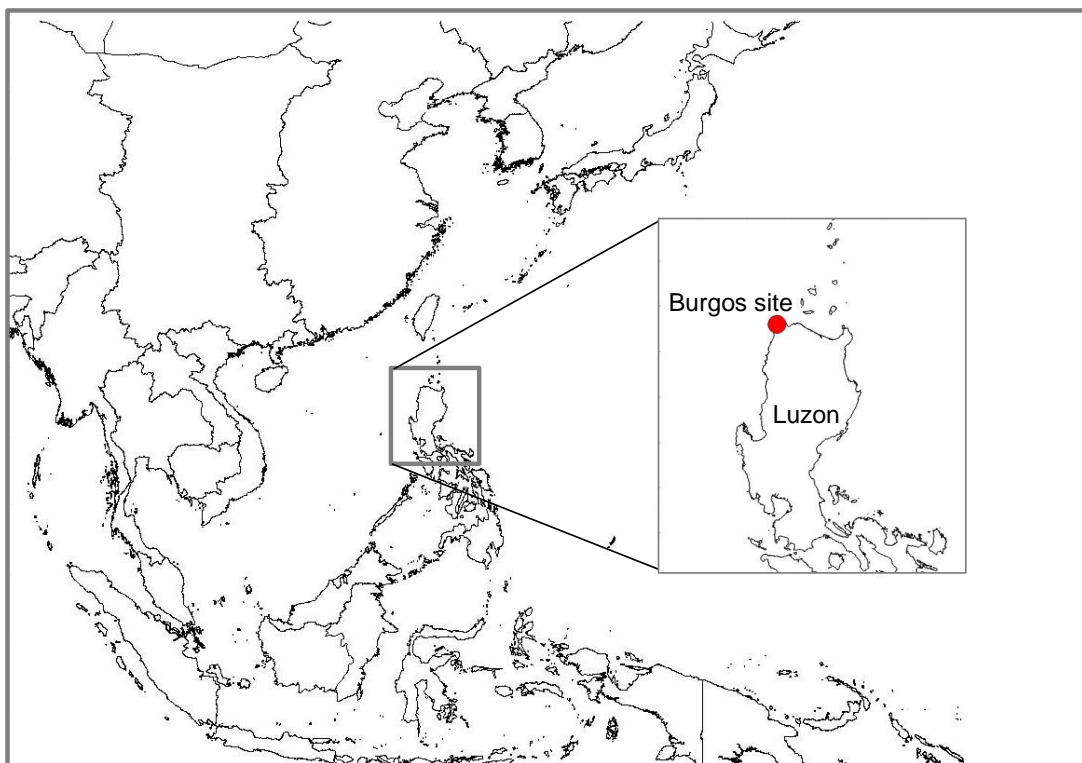
Figure 1. Map of East Asia, Southeast Asia and sampling site in Burgos, Philippines
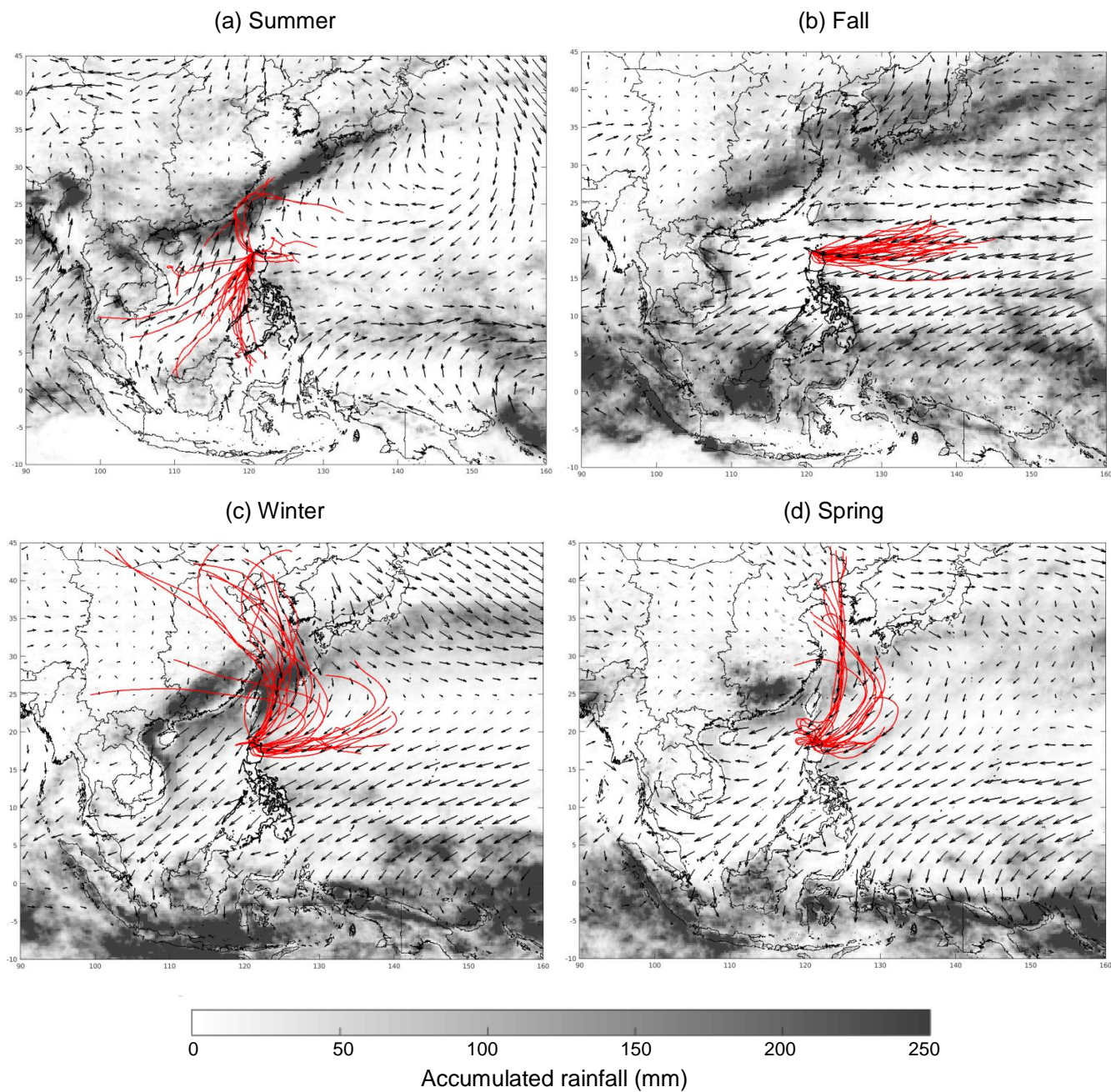
Figure 2. Wind (arrows), accumulated rainfall for each sampling period (shading, in mm) and wind back trajectory (red line) during a) summer, b) fall, c) winter and d) spring sampling season. The gray scale is white for a value of 0 and goes to black for a value of 250 in increments of 50mm.
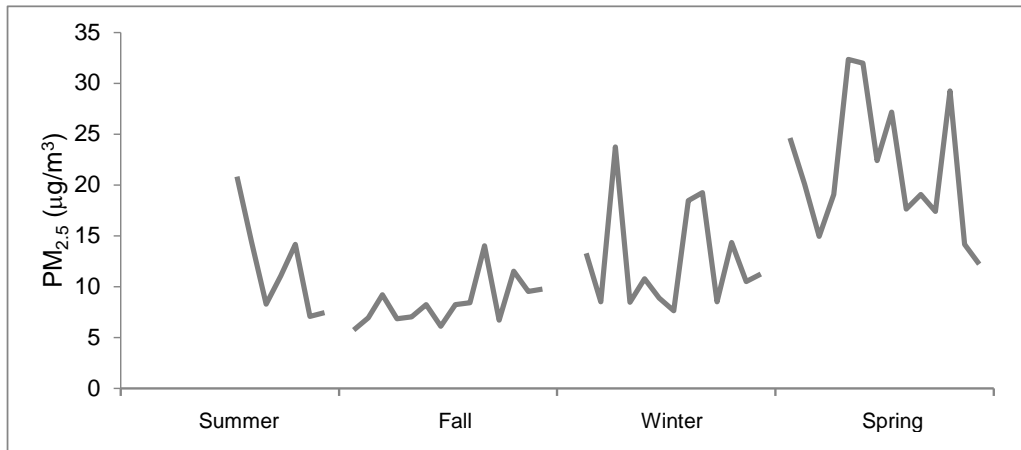
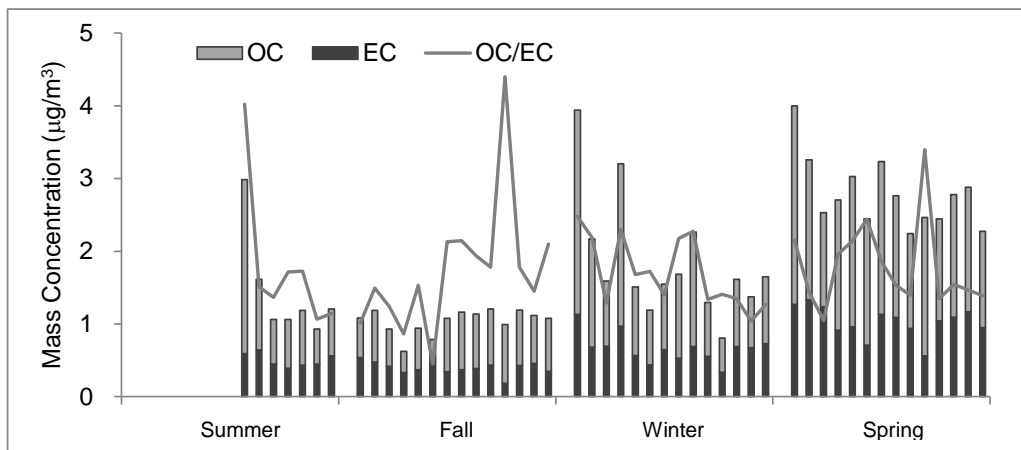**Figure 3.** Daily and seasonal variation of observed PM$_{2.5}$ mass concentration.

Figure 4. Daily Elemental Carbon (EC) and Organic Carbon (OC) mass concentration and OC/EC ratio.
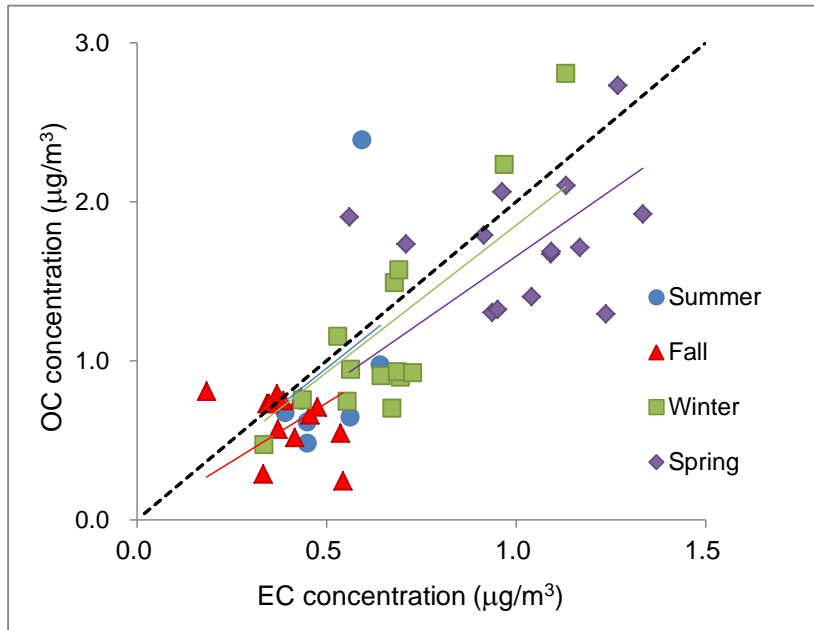
Figure 5. Scatterplot of OC and EC for summer, fall, winter and spring sampling period (in $\mu g\,m^{-3}$). Bold dashed line indicates OC/EC ratio of 2.
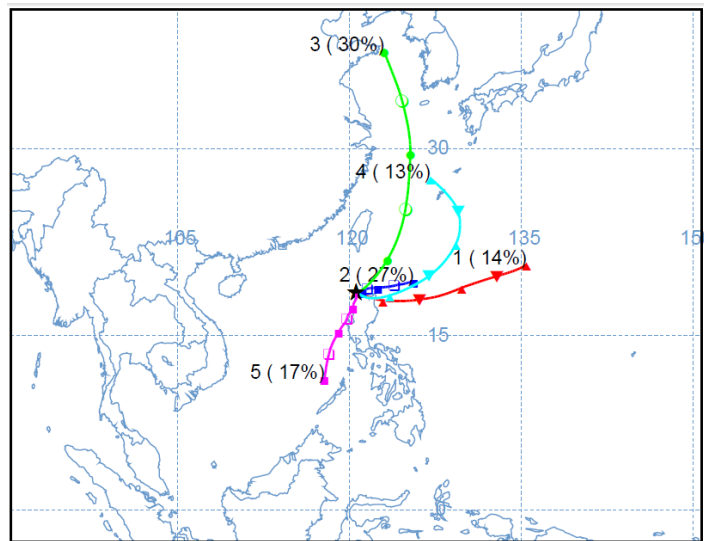

Figure 6. Cluster analysis of 72H HYSPLIT-WRF wind back trajectories arriving every 12 hours for each sampling day for all seasons. Color represents each of the 5 clusters generated by the analysis.
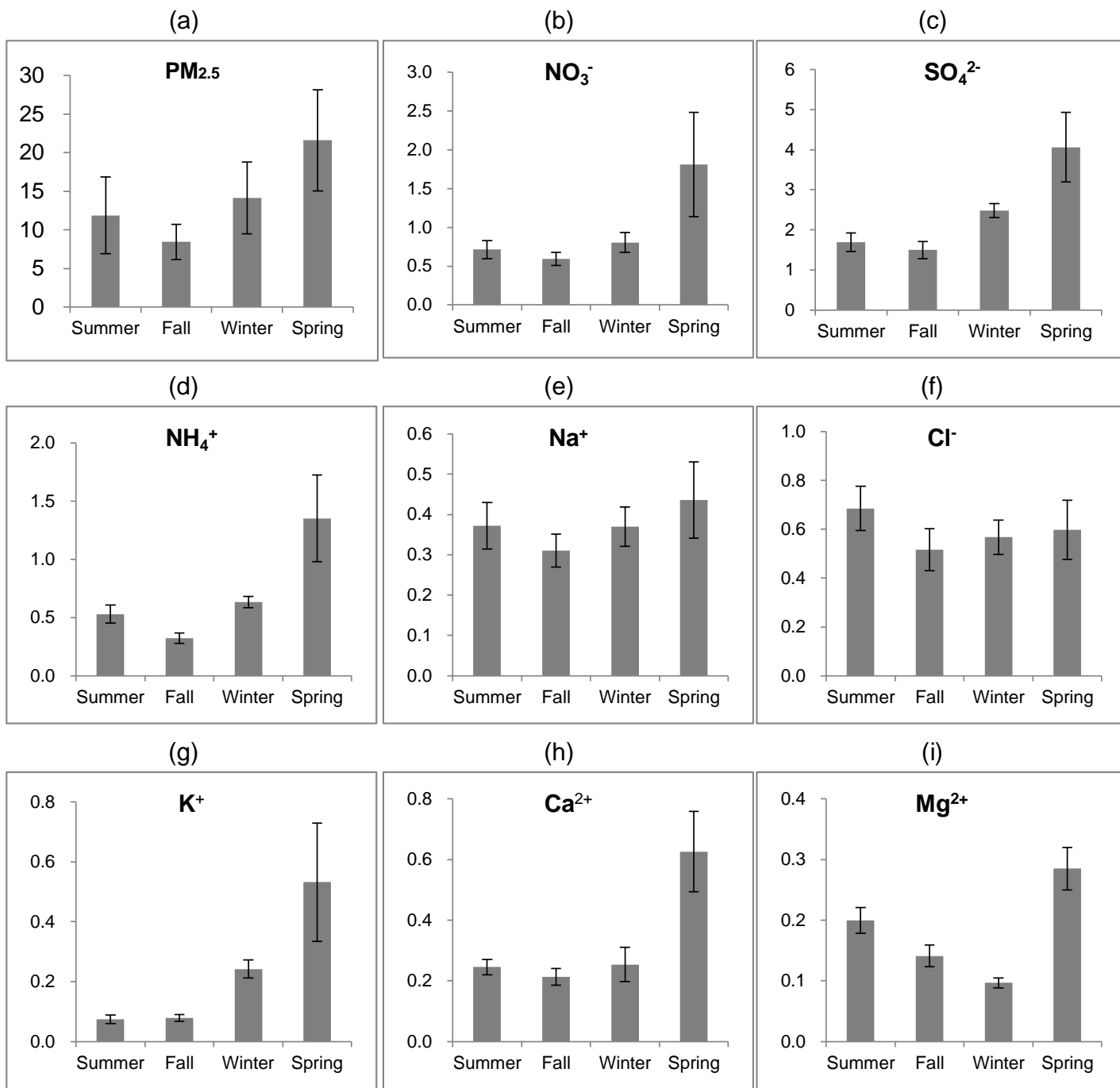
Figure 7. Seasonal mean mass concentration and standard deviation of (a) $PM_{2.5}$ and its ionic components (b) NO_3^-,(c) SO_4^{2-},(d) NH_4^+,(e) Na^+,(f) Cl^-,(g) K^+ ,(h) Ca^{2+} and (i) Mg^{2+} (unit in $\mu g\, m^{-3}$).
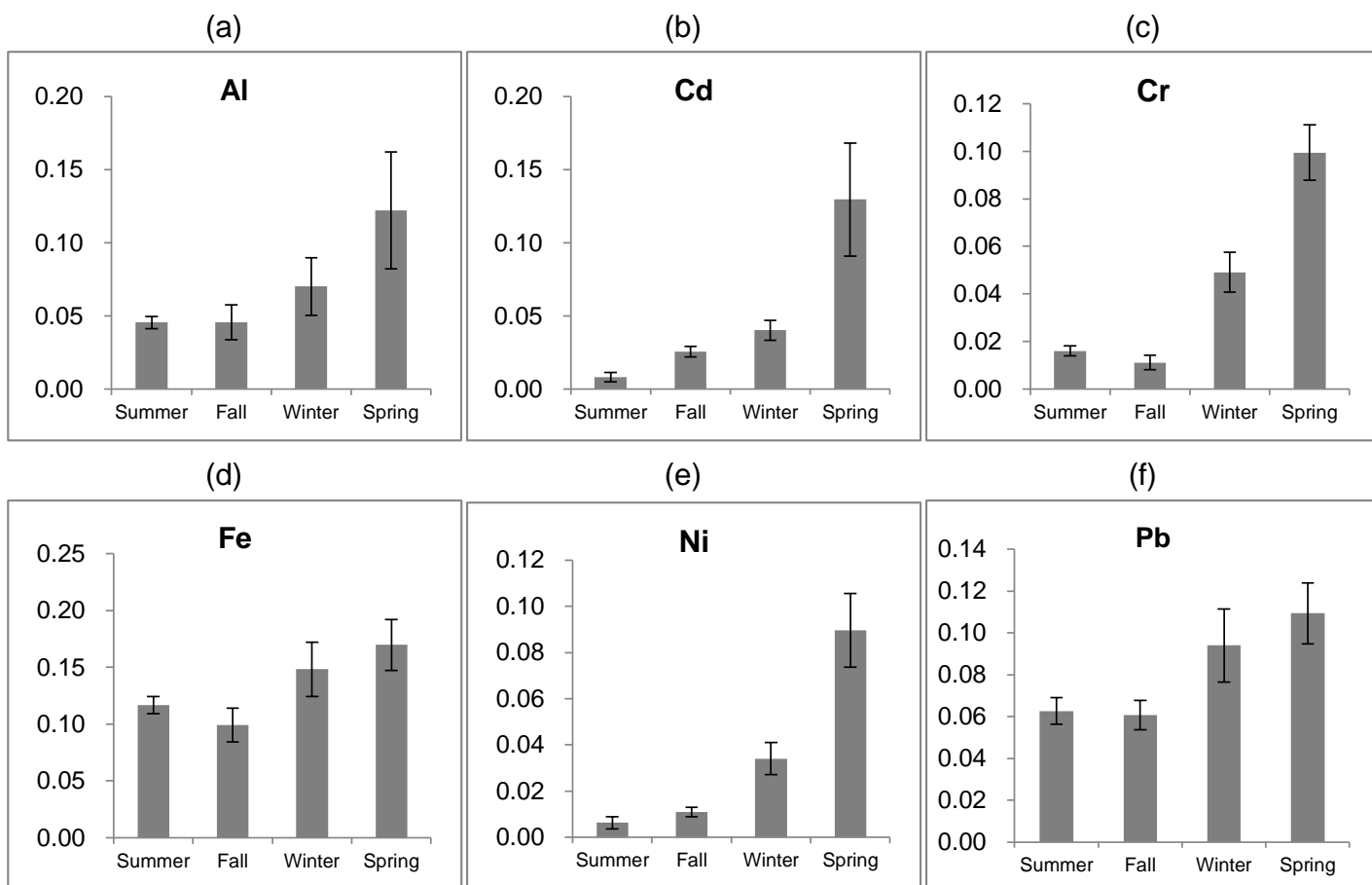
Figure 8. Seasonal mean mass concentration and standard deviation of metallic components (a) Al, (b) Cd, (c) Cr, (d) Fe, (e) Ni and (f) Pb (unit in $\mu g\, m^{-3}$).
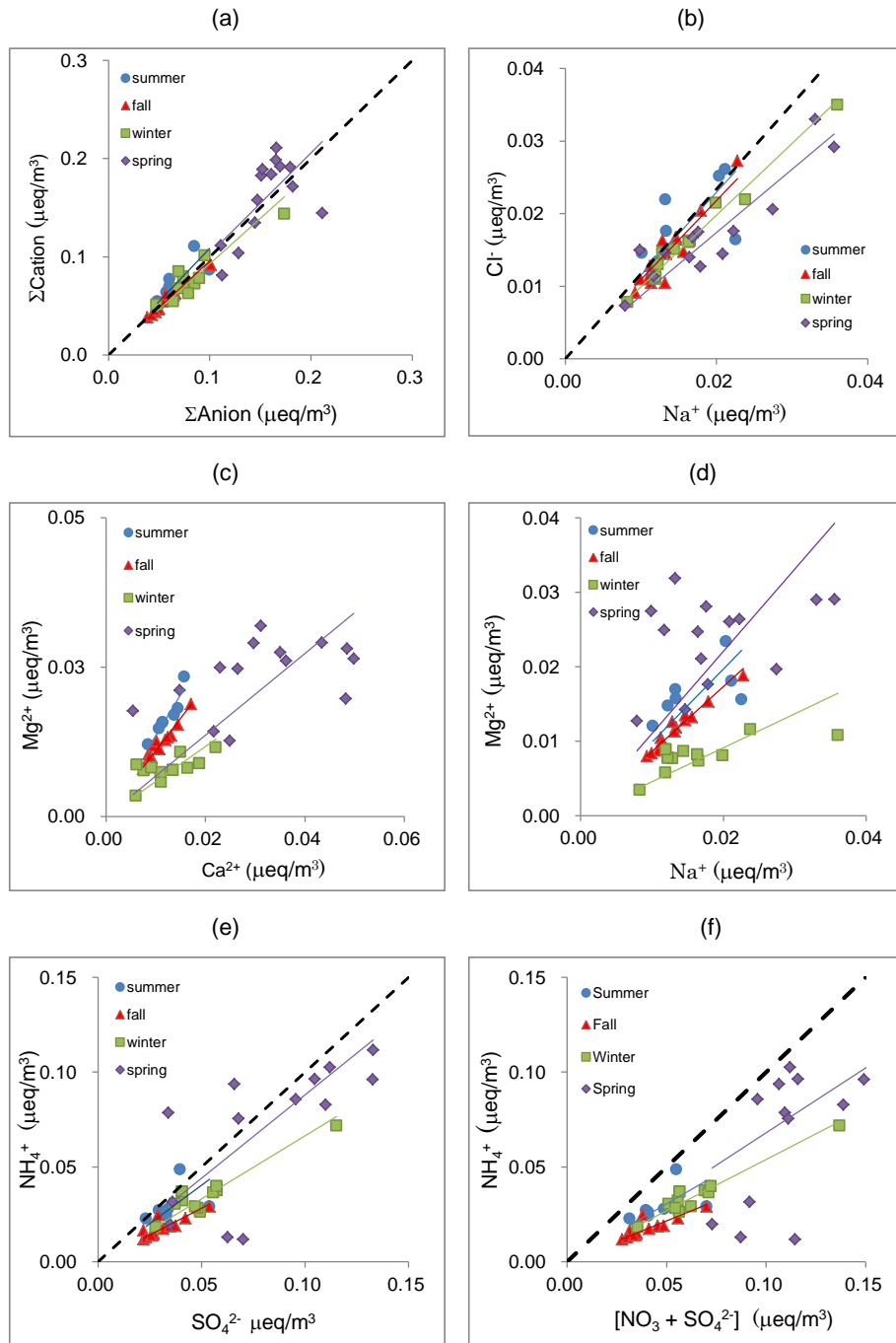
Figure 9. Scatter plot of a) total anion and cation, b) Na^+ and Cl^-, c) Mg^{2+} and Na^+, d) Mg^{2+} and Ca^{2+}, e) NH_4^+ and SO_4^{2-}, and f) NH_4^+ and $NO_3^- + SO_4^{2-}$ (unit in equivalent concentration).
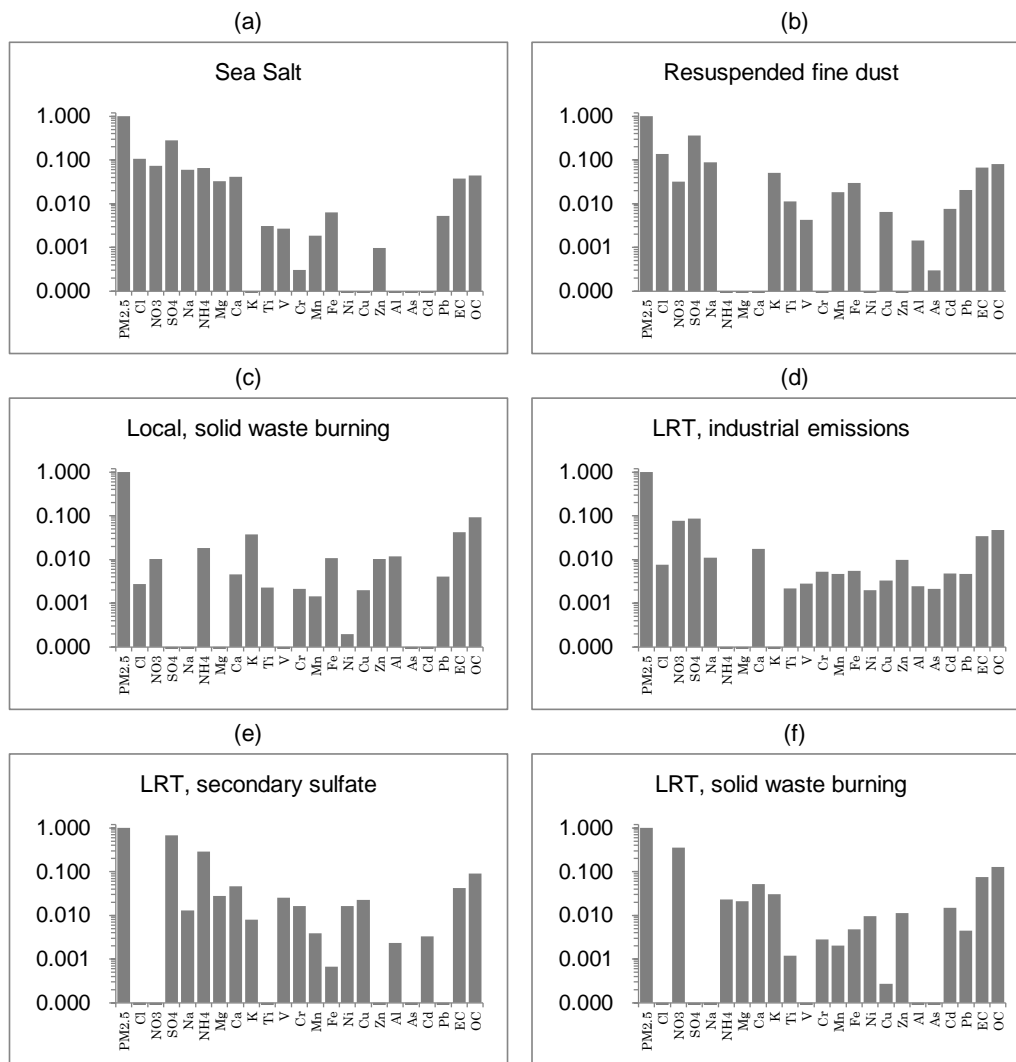
Figure 10. Source factor profiles from PMF analysis: (a) Sea Salt, (b) Resuspended fine dust, (c) Local, solid waste burning, (d) LRT, industrial emissions, (e) LRT, secondary sulfate and (f) LRT, solid waste burning.

Figure 11. Daily contribution for each source profile (a) Sea Salt, (b) Resuspended fine dust, (c) Local, solid waste burning, (d) LRT, industrial emissions, (e) LRT, secondary sulfate and (f) LRT, solid waste burning for all sampling period (unit is $\mu g\,m^{-3}$).
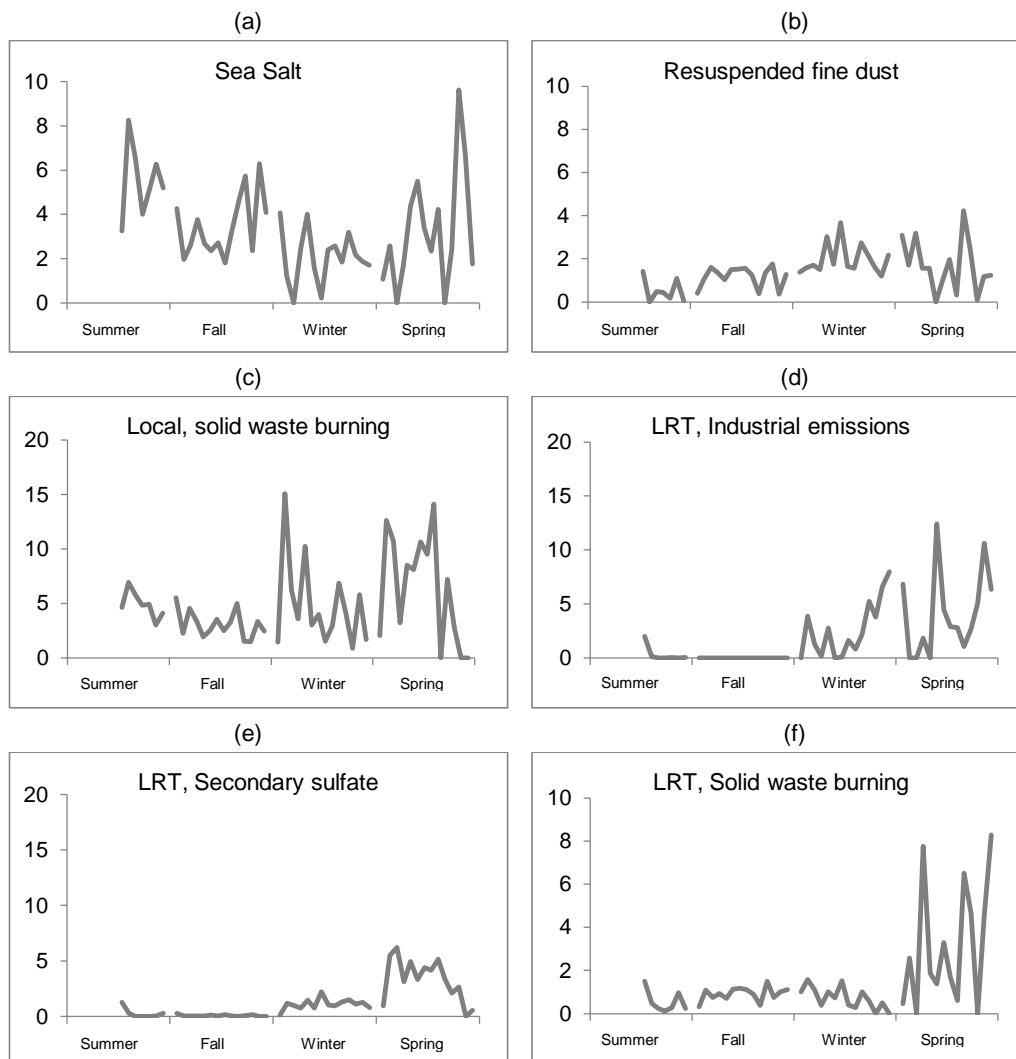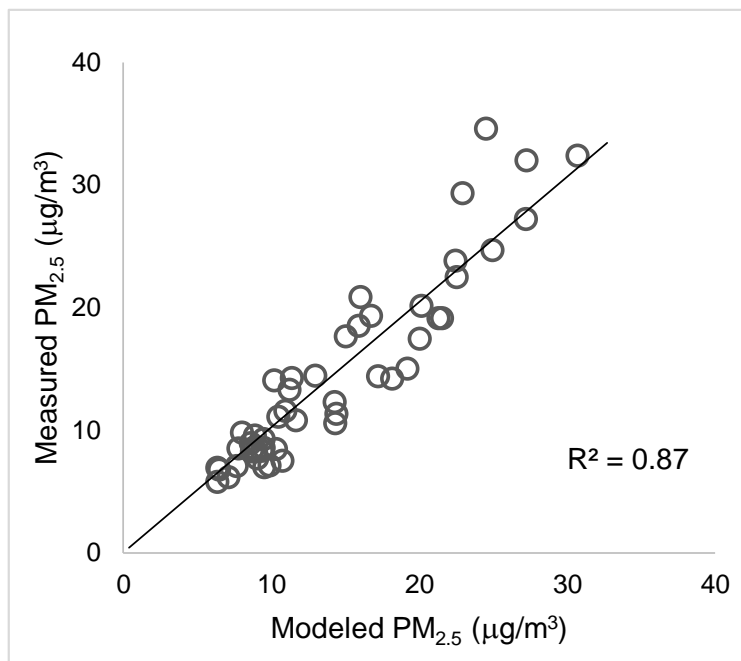
25

Figure 12. Measured vs. PMF model reconstruction of $PM_{2.5}$ mass concentration (unit is $\mu g\,m^{-3}$).

Table 2. Summary of mass concentration of $PM_{2.5}$ and its components (unit is $\mu g\,m^{-3}$).

	Summer	Fall	Winter	Spring
$PM_{2.5}$	11.9 ± 4.6	8.4 ± 2.2	14.2 ± 7.3	21.6 ± 6.6
EC	0.50 ± 0.09	0.40 ± 0.09	0.67 ± 0.19	1.03 ± 0.20
OC	0.93 ± 0.61	0.63 ± 0.17	1.18 ± 0.62	1.76 ± 0.37
NO_3^-	0.71 ± 0.21	0.60 ± 0.16	0.80 ± 0.27	1.81 ± 1.29
SO_4^{2-}	1.69 ± 0.43	1.50 ± 0.42	2.48 ± 0.94	4.06 ± 1.67
NH_4^+	0.53 ± 0.15	0.32 ± 0.09	0.63 ± 0.21	1.35 ± 0.72
Na^+	0.37 ± 0.11	0.31 ± 0.08	0.37 ± 0.15	0.44 ± 0.18
Cl^-	0.69 ± 0.17	0.52 ± 0.17	0.57 ± 0.23	0.60 ± 0.24
K^+	0.07 ± 0.03	0.08 ± 0.02	0.24 ± 0.07	0.53 ± 0.38
Ca^{2+}	0.25 ± 0.05	0.21 ± 0.05	0.25 ± 0.10	0.63 ± 0.26
Mg^{2+}	0.20 ± 0.04	0.14 ± 0.03	0.10 ± 0.02	0.29 ± 0.07
Al	0.05 ± 0.00	0.05 ± 0.01	0.07 ± 0.02	0.12 ± 0.04
Fe	0.12 ± 0.00	0.10 ± 0.02	0.15 ± 0.02	0.17 ± 0.02
Cd	0.01± 0.00	0.03 ± 0.00	0.04 ± 0.01	0.13 ± 0.04
Cr	0.02 ± 0.00	0.01 ± 0.00	0.05 ± 0.01	0.10 ± 0.01
Ni	0.00 ± 0.00	0.01 ± 0.00	0.03 ± 0.01	0.09 ± 0.02
Pb	0.06 ± 0.01	0.06 ± 0.01	0.09 ± 0.02	0.11± 0.01
Levoglucosan*	0.63 ± 0.86	1.4 ± 0.56	6.0 ± 2.4	19.1 ± 2.8

* unit in $ng\,m^{-3}$

Table 3. Summary of seasonal and annual source profile contribution (unit is $\mu g\,m^{-3}$).

Source	Summer	Fall	Winter	Spring	Annual
Sea salt	5.7 ± 1.5 (49%)	3.4 ± 1.4 (40%)	1.9 ± 1.1 (14%)	3.3 ± 2.6 (15%)	3.3 ± 2.1 (23%)
Resuspended fine dust	0.4 ± 0.4 (3%)	1.2 ± 0.4 (11%)	2.1 ± 0.7 (15%)	1.5 ± 1.2 (7%)	1.4 ± 1.0 (10%)
Local solid waste burning	5.0 ± 1.3 (43%)	2.8 ± 1.1 (33%)	4.8 ± 3.9 (35%)	6.2 ± 5.1 (29%)	4.7 ± 3.7 (33%)
LRT, industrial emission	0.02 ± 0.03 (0.1%)	0.0 ± 0.0 (0%)	3.1 ± 2.7 (22%)	4.0 ± 3.8 (18%)	2.0 ± 3.0 (14%)
LRT, secondary sulfate	0.1 ± 0.1 (1%)	0.1 ± 0.1 (1%)	1.2 ± 0.4 (8%)	3.3 ± 2.0 (15%)	1.3 ± 1.7 (9%)
LRT, solid waste burning	0.4 ± 0.3 (3%)	1.0 ± 0.3 (11%)	0.7 ± 0.5 (5%)	3.5 ± 2.8 (16%)	1.5 ± 2.0 (11%)

Table 4. Enrichment factors

	Solid waste burning		
	Local	LRT	
K^+/OC	0.4	0.2	
K^+/EC	0.9	0.4	
K^+/Zn	3.7	2.7	
K^+/NO_3^-	3.6	0.1	
	LRT episodes		
	Secondary sulfate	industrial	Resuspended fine dust
$(Ca^{2+}+Mg^{2+})$/Na^+	5.7	1.6	null
NO_3^-/SO_4^{2-}	null	0.9	0.1